Supporting Information

Anomalous Hall effect in edge-bonded monolayer graphene

Authors: Hui Liu[1, 4]*, Heng Wang[2]*, Zhisheng Peng[1, 4]*, Jiyou Jin[1, 4], Zhongpu Wang[1, 4], Kang Peng[1, 4], Wenxiang Wang[1, 4], Yushi Xu[1], Yu Wang[1], Zheng Wei[1, 4], Ding Zhang[2], Yong Jun Li[1, 3, 4]†,Weiguo Chu[1]†, Lianfeng Sun[1, 3, 4]†

Affiliations:

[1]*CAS Key Laboratory of Nanosystem and Hierarchical Fabrication, National Center for Nanoscience and Technology, Beijing 100190, China*

[2]*State Key Laboratory of Low Dimensional Quantum Physics and Department of Physics, Tsinghua University, Beijing 100084, China*

[3]*The GBA National Institute for Nanotechnology Innovation, Guangdong 510700, China*

[4]*University of Chinese Academy of Sciences, Beijing 100049, China*

†Correspondence authors. slf@nanoctr.cn (L.F.S.); wgchu@nanoctr.cn (W.G.C.); liyj@nanoctr.cn (Y.J.L.)

*These authors contributed equally to this work.

Supplementary Figures

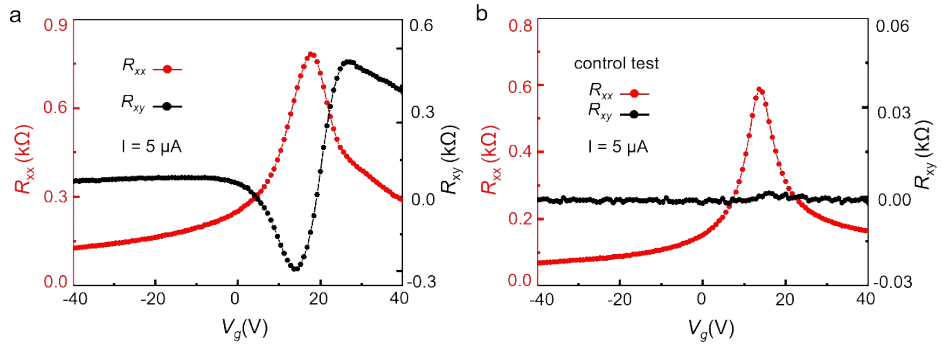

Figure S1. Comparison between a typical Hall resistance R_{xy} and longitudinal resistance R_{xx} with edge-bonded Hall bar (a) and that with usual Ti/Au Hall bar (b). Both are measured without external magnetic field at room temperature under atmospheric conditions. (**a**) R_{xy} (black) and R_{xx} (red) versus gate voltage V_g with edge-bonded Mo Hall bar. At zero external magnetic field, a non-zero R_{xy} obtained, which can be modulated with gate voltage V_g. This indicates clearly the existence of AHE and ferromagnetism. The Dirac point V_{Dirac} is found to be around 18.2 V from the peak position of R_{xx}. R_{xy} changes its sign around V_{Dirac}. (**b**) The Ti/Au (5/60 nm) electrodes of the Hall device were prepared by electron beam evaporation, which do not have edge-bonded Hall bar structure. R_{xy} (black) and R_{xx} (red) are shown for this kind of Ti/Au Hall bar device without external magnetic field. The result that R_{xx}~V_g curve has a peak is attributed to the charge neutral point of graphene. R_{xy}~V_g curve in Figure S1b is a flat line and R_{xy} has a value around zero, indicating no Hall effect without the external magnetic field.

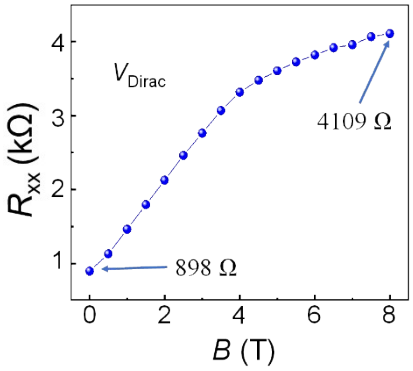

Figure S2. Longitudinal resistance R_{xx} as a function of the magnetic field B at V_{Dirac} extracted from Figure 2C in the main text (temperature: 150 K). A positive and

linear MR of R_{xx} is observed in the magnetic field range of 0~4.0 T. When the magnetic field increases from 4.0 to 8.0 T, the MR shows a tendency to saturate and reaches a maximum value ~358 %. This suggests a potential quantum-mechanical origin due to the charge neutral nature at the Dirac point.

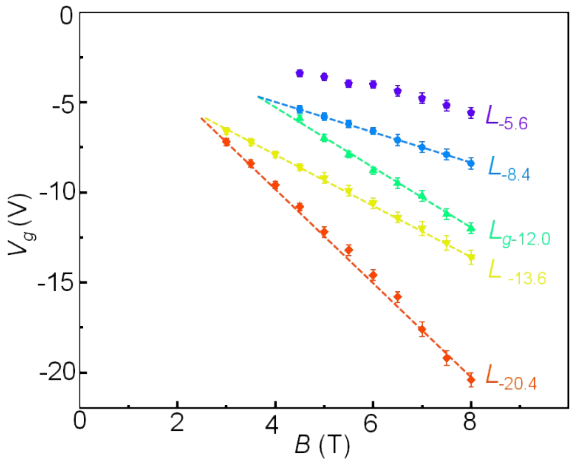

Figure S3. Values of V_g of the peaks and valleys of R_{xx} as a function of the magnetic field *B*. At magnetic field of 8.0 T, typical values of the peaks and valleys of V_g are shown in the above figure, which are -20.4, -13.6, -12.0, -8.4 and -5.6 V, respectively. The dependence of these V_gs on the magnetic field is almost linear as shown here. The two lines of $L_{-20.4}$ and $L_{-13.6} \propto B$ intersect at a magnetic field of ~ 2.5 T. Here $L_{-20.4}$ represents the straight line starting at V_g = - 20.4 V, etc. And the two lines of $L_{-12.0}$ and $L_{-8.4}$ intersect at a magnetic field of ~ 3.5 T. This suggests a mechanism induced by high magnetic fields, which is attributed to Zeeman splitting of the Landau Level.

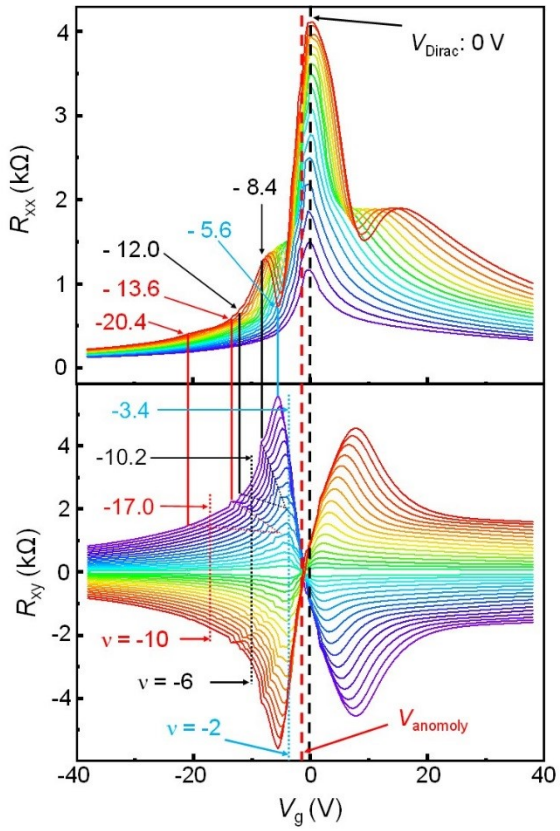

Figure S4. Calculation of the filling factors.

The hole concentration in graphene can be calculated by the following formula: $n_h=1/(R_H\ e)$. Here n_h is the hole concentration, e is the electron charge and R_H is Hall coefficient. For the graphene Hall device 1 [Figure 2(d) in the main text], the hole concentrations, which can be obtained from Hall resistance, are 1.92×10^{16}, 1.25×10^{16} and 3.98×10^{15} m^{-2}, at gate voltages of -17.0, -10.2 and -3.4 V, respectively.

Thus, the filling factor ν is calculated with the following equation:

$$\nu(V_g) = n(V_g)\frac{h}{eB}$$

Where V_g, $n(V_g)$, h, e, B represent the gate voltage, hole concentration, Planck's constant, electron charge and magnetic field strength, respectively. The fill factors ν correspond to -2, -6, -10 at gate voltages of -3.4 V, -10.2 V and -17.0 V for the magnetic field of 8.0 T, respectively.

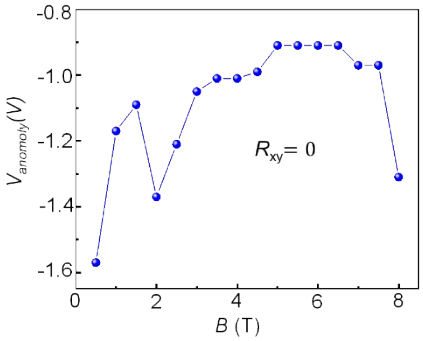

Figure S5. $V_{anomaly}$ as a function of the magnetic field. The Hall resistance R_{xy} becomes zero at the gate voltages, which is named $V_{anomaly}$. From this figure, it can be seen that $V_{anomaly}$ shows dependence on the magnetic field with an oscillatory structure. The smallest (-1.58 V) and largest (-0.90 V) of $V_{anomaly}$ correspond to a magnetic field of 0.5 T and to a range of magnetic field 5.5 ~7.0 T, respectively. This means that $V_{anomaly}$ is in a very narrow range of 0.68 V. The origin and mechanism of this $V_{anomaly}$ is attributed to the ferromagnetism in pristine monolayer graphene, which has been discussed and explained in the main text.

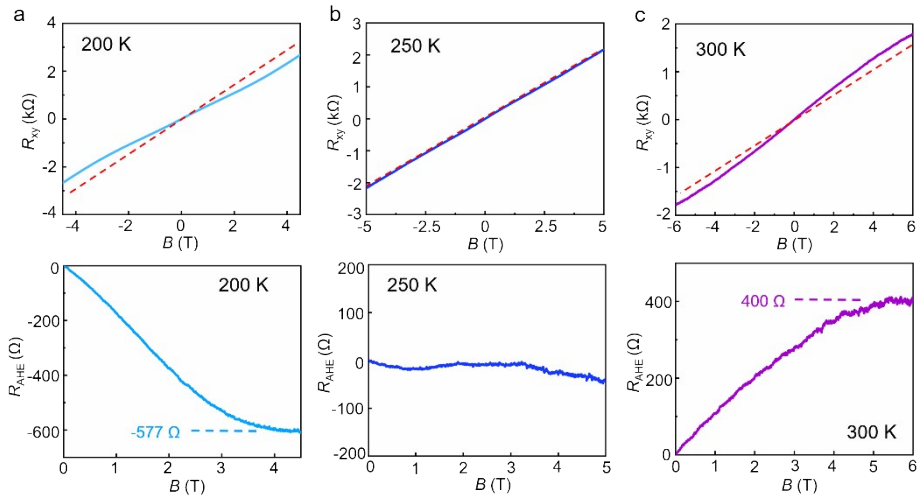

Figure S6. Hall resistance R_{xy} and anomalous Hall resistance R_{AHE} versus the magnetic field B. (**a**) R_{xy} and R_{AHE} as a function of the magnetic field B at temperature of 200 K. The blue curve represents the Hall resistance R_{xy}, exhibiting nonlinearity. The dash straight line represents the contribution from normal Hall effect. At 200 K, it takes a magnetic field ~4 T for R_{AHE} to reach saturation. (**b**) A linear relation between R_{xy} and the magnetic field B at temperature of 250 K. This suggests that R_{AHE} has a value close to zero. (**c**) Hall resistance R_{xy} versus the magnetic field B at temperature of 300 K. The purple curve represents R_{xy} and the dash straight line represents the contribution from normal Hall effect, i.e., $R_{xy} = \alpha B + \beta M$. Here, β exhibits a reversal of its sign comparing to that in 200 K.

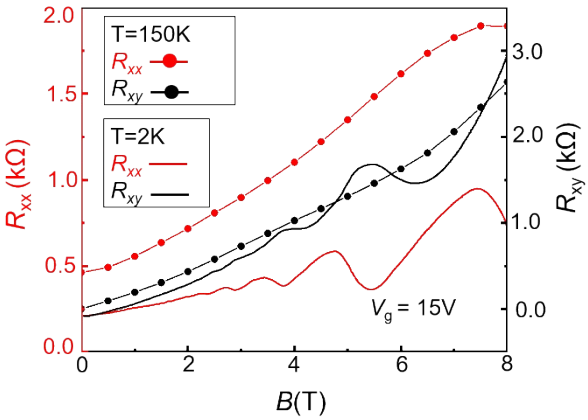

Figure S7. Dependence of R_{xy}, R_{xx} on the magnetic field at temperature of 2 and 150 K at fixed gate voltage of 15 V. This device is the same one as that shown in Figure 2 in the main text (device 1). In this figure, there are two sets of curves: one represents that of R_{xy} and R_{xx} at temperature of 150 K, and the other for that at temperature of 2 K. For R_{xy} and R_{xx} at temperature of 150 K, the two curves have the same trend; while R_{xy} and R_{xx} have opposite trend at temperature of 150 K around 5 T. This phenomenon may be explained as an early indication of quantum Hall effect, when pronounced plateau-like features are observed in R_{xy} while R_{xx} exhibits pronounced Shubnikov de Haas oscillations.

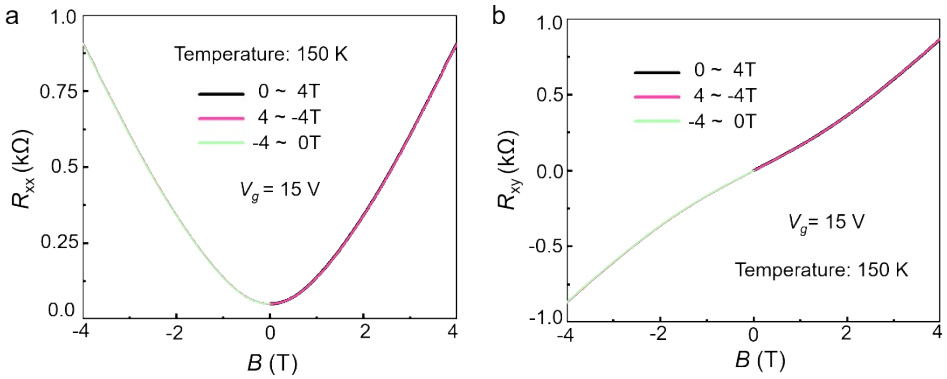

Figure S8. R_{xx} and R_{xy} as a function of the magnetic field when the field is swept up and down at a rate of 0.001 T/second. The device is the same as that shown in Figure 2 in the main text (device 1) and the temperature is 150 K. (**a**) R_{xx} versus the magnetic field B. (**b**) R_{xy} versus the magnetic field B. The magnetic field is first swept up from 0

to 4 T; then, it is swept down from 4 to -4 T. At last, the field is swept up from -4 to 0 T. The curves are coincident and no hysteresis loops are observed.

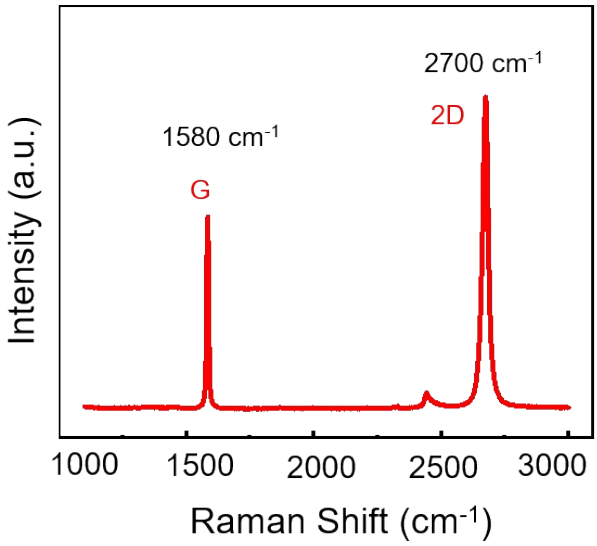

Figure S9. Raman spectra of a typical graphene prepared by mechanical stripped method in our work.

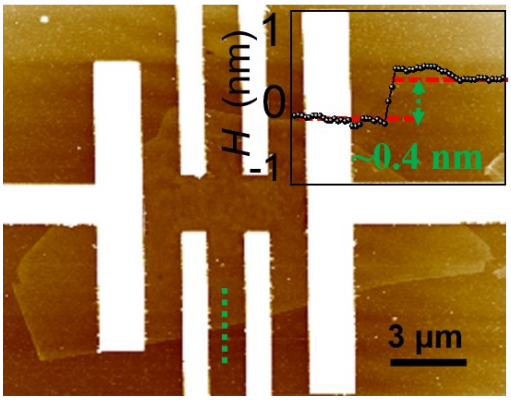

Figure S10. AFM topography of the graphene Hall bar device, the inset shows the height variation along the green dashed line.

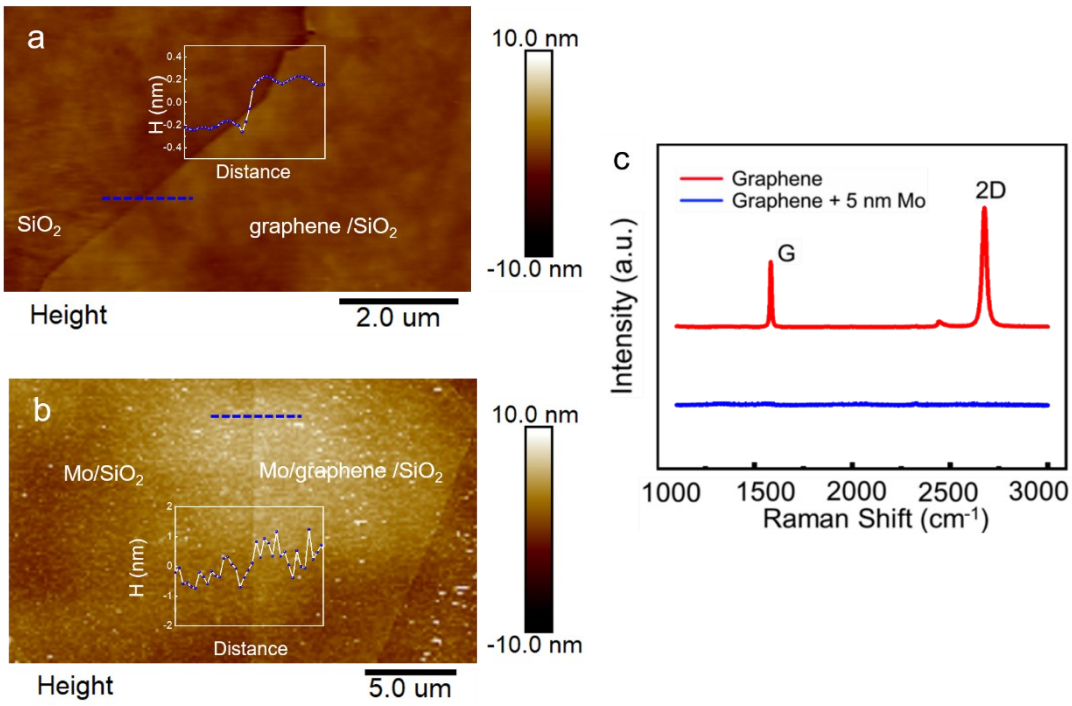

Figure S11. AFM topography of (**a**) a monolayer graphene on silicon substrate and (**b**) a monolayer graphene covering 5 nm Mo on silicon substrate. The insets show the height variation along the blue dashed line. (**c**) Comparison of the Raman spectra of the monolayer graphene in (a) with the monolayer graphene covering 5 nm Mo in (b).

The 5 nm Mo was deposited with magnetron sputtering (Lesker Lab 18) at the pressure of 10^{-5} torr and the power of 150 W. We have measured the corresponding AFM topographic image. Figure S11a shows the AFM image of the pristine graphene which has a height difference of ~0.4 nm comparing to the substrate. AFM image of a monolayer graphene after covering 5 nm Mo is significantly different as shown in Figure S11b compared with the monolayer pristine graphene. Together with the Raman spectrum in Figure S11c, it is believed that a solid-solid reaction occurs between the graphene and Mo atoms rather than a physical stacking of Mo on graphene.

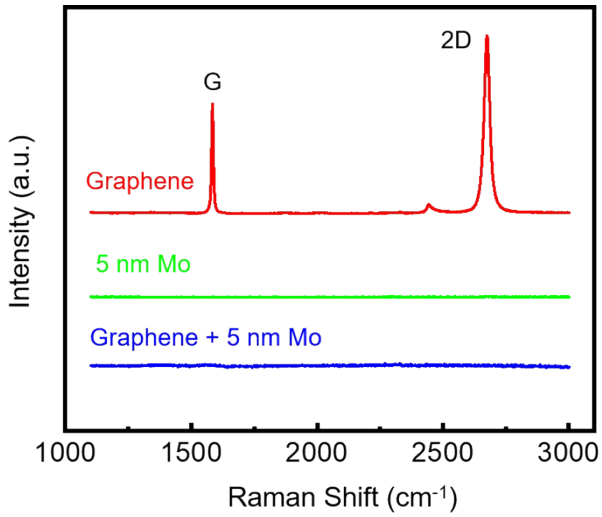

Figure S12. Comparison of the Raman spectra of monolayer graphene, 5 nm Mo and graphene covered with 5 nm Mo.

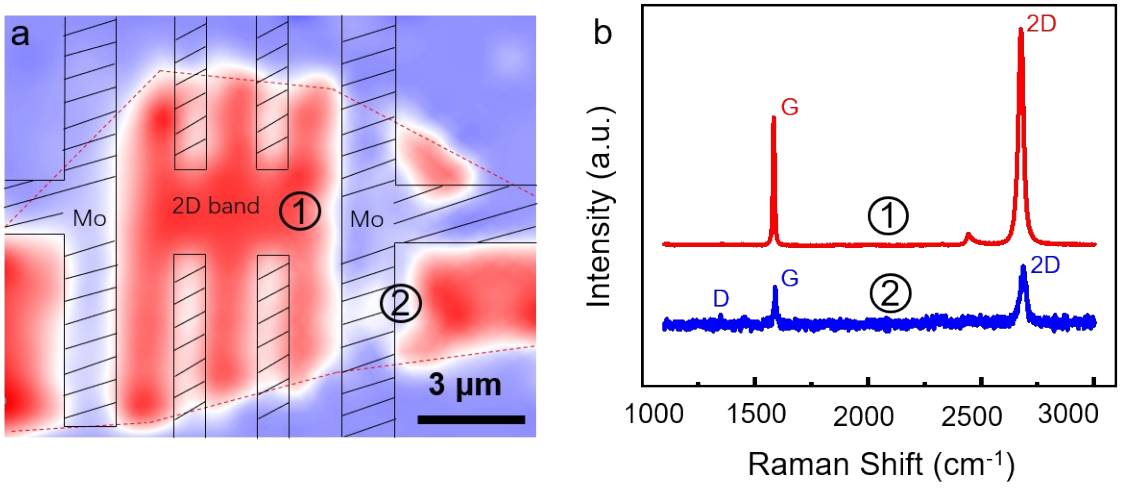

Figure S13. (**a**) Scanning Raman spectroscopic map plotting 2D band of graphene for Hall bar device. It can be seen that 2D-peaks are clearly present in the graphene except the position below the Mo electrode. (**b**) Raman spectra of graphene at the annotated position in (a). Decreasing of the intensity of the Raman characteristic peak can be observed close to the edge of the molybdenum electrode, and a weak D peak appears. It is believed that a solid-solid reaction occurs between the graphene and Mo atoms rather than a physical stacking of Mo on graphene.